

S & M 0747

Gettering by CF₄-Ar Plasma-Treated Titanium within Anodically Bonded Glass-Silicon Microcavities

Surajit Kumar Hazra, Nam-kuk Kim, Jaehong Park, Byoungdoo Choi, Sangmin Lee, Tae-young Choi and Dong-Il “Dan” Cho*

ISRC/ASRI, School of Electrical Engineering and Computer Sciences, Seoul National University, San 56-1, Shinlim-dong, Kwanak-gu, Seoul 151-742, Korea

(Received May 7, 2008; accepted September 29, 2008)

Key words: getter, titanium, plasma, fluorine, anodic bonding, XPS

The gettering of CF₄-Ar plasma-treated titanium films has been studied by X-ray photoelectron spectroscopy, optical microscopy and field emission scanning electron microscopy. This study shows a convenient way to eliminate the native oxide impurities from the titanium surface before getter activation. A vacuum-packaged environment and the activation conditions for 2 mm × 1.8 mm × 2500 Å titanium getter films were realized by a glass-silicon anodic bonding process at 400°C and a 40 min thermal treatment at 500°C, respectively. The surface characteristics of the titanium films were analyzed before and after packaging to determine the role of fluorine. The fluorine coverage on the titanium surface as a result of plasma treatment reveals a new gettering mechanism with high oxygen-capturing potential.

1. Introduction

Getters are important components in vacuum-packaged devices.⁽¹⁻⁴⁾ Sometimes they are called micro-/macro-vacuum pumps because they can control *in situ* the level of vacuum within packaged devices without external pumping. A simple way to define gettering is the removal of atoms and molecules from the gas phase by physisorption and chemisorption on an active material surface. As a matter of fact, the mechanism of gettering is related solely to the surface reactivity of the material, and a direct proportionality between gettering and active surface area is obvious. However, enhancing surface activity without increasing the geometrical area of a material's surface is challenging and is the current goal for microgetters within vacuum-packaged devices.

Vacuum packaging of microchips with getters involves a sequential process flow and often the getter is exposed to the laboratory atmosphere after deposition and before the final hermetic sealing step. This leads to surface contamination resulting in the

*Corresponding author: e-mail: dicho@snu.ac.kr

development of a native contaminant layer on the active surface of the getter where it remains permanently as an unwanted impurity. Although the native contaminant layer may be thin, it is apparent that surface activity is likely to be reduced. The conventional way to deal with this native impurity layer is to activate the getter with a heat treatment in high vacuum in the temperature range from 400 to 600°C to regenerate the active surface.⁽⁵⁾ The underlying mechanism of activation is desorption of impurities from the getter surface as well as dissolution of impurities into the bulk getter, and its success depends on factors such as vacuum level, ambient temperature, and the nature of impurities. As a result, the activation temperature is different for different gettering materials. Thus, various successful attempts have been made to lower this activation temperature by altering the getter composition,^(6,7) but reports on the elimination of the native impurity layer before packaging are rare.

Titanium (Ti) is a versatile material for different applications. Some important areas where this metal has been used are in biomedical and metallurgical devices and components.^(8,9) Owing to its chemical properties, Ti and Ti alloys are widely used getter materials in vacuum devices.⁽¹⁰⁻¹²⁾ The gettering activity of titanium is a chemical process and active gases, such as H₂, CO, CO₂, N₂, O₂, and H₂O, are sorbed on activated titanium surfaces by simple chemical reactions. However, if the reaction sites on which gas molecules land are occupied, they probably return to the gas phase, so the cleanliness of the surface plays a very important role in the pumping speed of a titanium getter.

Wet chemical techniques are sometimes used to clean titanium surfaces. In the case of untreated titanium or titanium heat-treated below 600°C, the surface can be cleaned by treating the metal with a mixture of nitric acid (HNO₃), hydrofluoric acid (HF), and DI water at 54°C.⁽¹³⁾ Although this technique is useful for removing oxides and other impurities, the surface may pick up some fluoride contaminants. To eliminate the fluoride contaminants, subsequent annealing at high temperatures is necessary.⁽¹⁴⁾ However, this technique is not suitable for titanium getters used in packaged MEMS devices. The main reason for this is that the substrate glass wafer (for titanium) is vulnerable to HF attack at 54°C. Even if masking techniques are used to protect the glass, the process will thereby be complicated and processing costs and the probability of further titanium contamination will increase. Dry etching techniques, such as reactive ion etching (RIE) and plasma etching, are more effective than wet etching methods for treating pure metal or alloy surfaces in micromachining technology.

In this paper, we report on the gettering of plasma-treated titanium. The titanium surface will have been exposed to reactive CF₄-Ar plasma before packaging. It has been shown that this plasma treatment removes native impurities from the titanium surface and creates a protective fluoride layer, which escapes before glass-silicon anodic bonding. The surface characteristics of titanium have been systematically examined with the help of X-ray photoelectron spectroscopy (XPS), optical microscopy, and field emission scanning electron microscopy (FE-SEM) for chemical-state information, colour, and morphological features, respectively. The results are discussed in detail in the context of the gettering mechanism. To the best of our knowledge, this is the first report on the gettering characteristics of plasma-treated titanium.

2. Materials and Methods

Four-inch Pyrex # 7740 glass wafers (thickness $\sim 350 \mu\text{m}$) were the starting material for this study. The first step was to fabricate cavities on the Pyrex glass wafers. For this, amorphous silicon, the masking material for the wet etching of glass, was deposited on both sides of the glass wafers using low-pressure chemical vapour deposition (LPCVD) equipment. The process temperature inside the CVD reactor was set at 550°C , and the ambient pressure was maintained at 300 mTorr with a constant flow of 60 sccm silane (SiH_4) gas. These deposition conditions were maintained for 80 min to deposit 2000 \AA of amorphous silicon on the glass wafers (Fig. 1(a)). After deposition, the glass wafers were patterned on one side for the cavity wet etching process (Fig. 1(b)). The pattern size on the mask was $1750 \mu\text{m} \times 2000 \mu\text{m}$. The patterned glass wafers were then etched in 49% HF solution to obtain $200\text{-}\mu\text{m}$ -deep cavities (Fig. 1(c)). The cavity depth was confirmed from α -step measurements performed on the etched glass surface after complete removal of the amorphous silicon in tetramethylammonium hydroxide (TMAH) solution (Fig. 1(d)). The final opening size of a cavity after wet etching was approximately $2.37 \text{ mm} \times 2.11 \text{ mm}$.

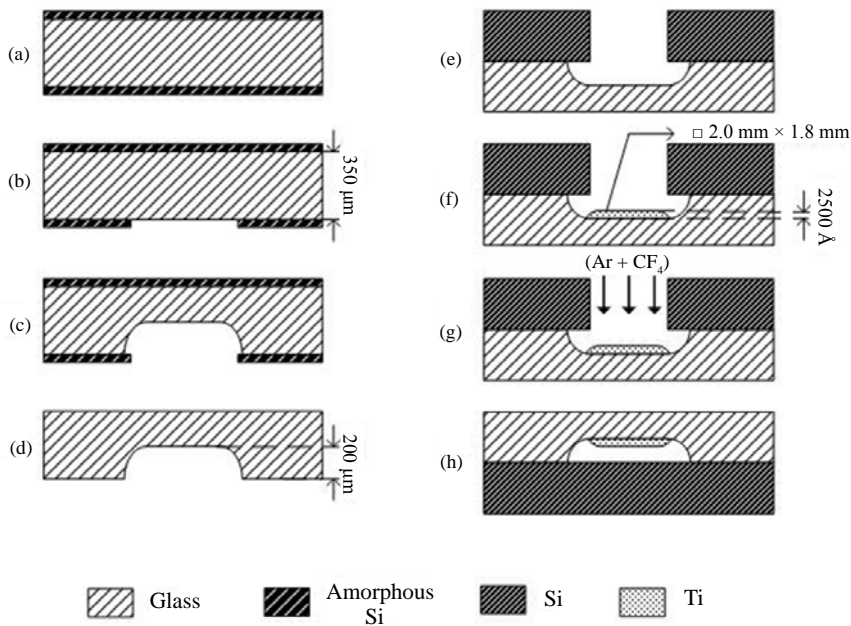


Fig. 1. Fabrication and packaging process flow: (a) Amorphous silicon is deposited on glass wafer; (b) amorphous silicon is patterned; (c) cavities are fabricated by wet etching in hydrofluoric acid solution; (d) amorphous silicon layer is removed in tetramethylammonium hydroxide (TMAH) solution; (e) silicon shadow mask and glass wafer are coupled; (f) titanium is deposited; (g) titanium is treated with plasma; (h) glass and silicon wafers are anodically bonded after thermal outgassing in vacuum.

After the cavities were fabricated, the glass wafers were thermally treated for 5 h in vacuum (10^{-4} Torr) to eliminate moisture and adsorbed gaseous impurities picked up during the wet fabrication process. The treatment started at 100°C and the temperature was raised to 400°C (in increments of 50°C), followed by natural cooling to room temperature. Then, the wafers were coupled to silicon shadow masks and introduced into the electron beam evaporation chamber for selective titanium deposition (Figs. 1(e) and 1(f)). High-purity titanium (99.95%, RND Korea) was used for the deposition process, and the wafers were rotated during deposition for uniformity. As observed under an optical microscope, the deposited titanium area was approximately $2\text{ mm} \times 1.8\text{ mm}$. The α -step profile of deposited titanium on a separate piece of plain glass revealed a thickness of 2500 \AA .

The plasma treatment on some of the titanium-deposited glass wafers was carried out using an Oxford etcher (Model: RIE 80 plus). The reactive plasma composition used for this purpose was a mixture of 60% tetrafluoromethane (CF_4) and 40% argon (Ar). Titanium was etched for 1 min after the plasma was generated with 200 W applied RF power and 0.1 Torr chamber pressure (Fig. 1(g)).

For getter packaging, the glass wafer was bonded to a silicon wafer at 400°C inside an EV 501 Bonder (Electronic Vision Co., Austria) (Fig. 1(h)). Optical wafer alignment prior to bonding was not necessary because of the use of bare silicon wafers. The bonding procedure was a computer-controlled sequential process flow. Initially, the wafers were thermally treated in vacuum and high-purity argon atmosphere to ensure complete outgassing of adsorbed moisture and gaseous impurities from the inner cavity surface.⁽¹⁵⁾ This was the second outgassing event required before the final hermetic sealing step. The starting temperature for outgassing was 100°C , after which the temperature was increased to 150°C followed by cooling to 70°C . Then, the temperature was again raised to 100°C , 150°C , 200°C , and 250°C . During this process, the pressure was maintained at 10^{-4} Torr, and at each temperature, argon purging was performed twice to purify the atmosphere between the wafers. The time delay between two temperatures was 30 min. Finally, the temperature was increased to 400°C (the bonding temperature). At 400°C , the pressure was set at 10 mTorr with argon purging. The temperature and pressure values were allowed to stabilize for another 30 min. A 200 N force was then applied on top of the wafers for proper contact, and subsequently, 650 V was applied to complete the bonding process. After completing the hermetic sealing, the temperature was again raised to 500°C for getter activation (or getter firing). The activation temperature was maintained at 500°C for 40 min, and then, the system was allowed to cool to room temperature.

The samples for analysis were obtained from the bonded wafers by dicing (DISCO, Japan; Model: DAD 522). Hair-line dicing patterns (depending on the size of the getter) were made on the wafers to separate the getter area from the rest of the wafer. After dicing, the samples were collected manually with the utmost care.

Elemental chemical-state information from the getter surface was obtained by X-ray photoelectron spectroscopy (Sigma Probe, Thermo VG, UK). The measurements were performed with an $\text{Al K}\alpha$ (1486.6 eV) X-ray source. Argon ion-sputter etching was also performed to ensure that the spectra came from clean surfaces without atmospheric contaminants.

The colour of the samples was investigated using an optical microscope, and the surface morphology of the samples was studied by FE-SEM (Hitachi, Model: S-48000).

3. Results

3.1 X-ray photoelectron spectroscopy

In this study, the XPS instrument was not coupled to the experimental processing chamber. The samples are likely to develop a protective native impurity layer on the surface owing to atmospheric exposure when they are taken out of the processing chamber.⁽¹⁶⁾ Since XPS is an extremely surface-sensitive technique, this unwanted native layer modifies the surface spectra to a large extent and the actual surface information is perturbed. This hinders quantitative estimation of the gettered amount. Consequently, an indirect approach was used to reveal the real surface and to highlight the differences due to this native impurity layer.

Figure 2 shows three $2p$ spectra of plasma-treated titanium obtained from the same sample surface under different conditions. The dashed line (I) is the spectrum of a plasma-treated Ti surface after unloading the sample from the plasma chamber and then reloading it in the XPS chamber. This involves exposure of the sample to the atmosphere. The solid line (II) is the spectrum obtained after *in situ* removal of the native impurity layer by Ar^+ ion-sputter etching. The dotted line (III) is the spectrum obtained after exposing the argon-cleaned surface to the atmosphere for 10 min. It is evident from Fig. 2 that spectra I and III are congruent, while II is distinct and located on the higher binding energy side. The interpretation of this observation is based on the fact that an active metallic surface develops a protective layer (mainly native oxide) when it comes in contact with the atmosphere. Hence, III will revert back to I because the Ar-cleaned surface has been exposed to the atmosphere and both have native oxide on their surfaces. Therefore, I and III are apparently spectra of the same surface. This

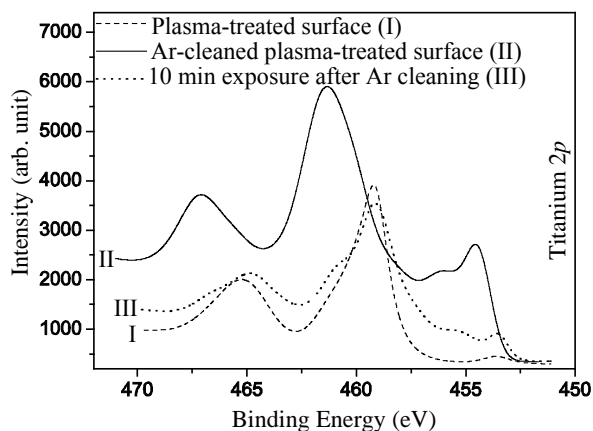


Fig. 2. Effect of native impurities on the XPS spectrum of plasma-treated titanium.

implies that the intermediate measurement II must reveal the real CF_4 -Ar plasma-treated surface. The shift of II towards the higher binding energy side is due to the effect of electronegative fluorine, which is discussed later in this report. In this study, we considered the spectrum from the Ar-cleaned surface for analysis.

The Ti $2p$ XPS spectra obtained after plasma treatment and after packaging and firing the plasma-treated titanium are shown in Figs. 3(A) and 3(B), respectively. The corresponding fluorine spectra (F $1s$) for the above two categories of titanium are shown in Figs. 3(a) and 3(b). The symbols S1 and S2 are used in each figure to indicate the as-prepared surface and the surface after *in situ* removal of the native oxide by Ar^+ sputter etching, respectively.

In the case of plasma-treated titanium, the S1 spectrum depicts mainly the native oxide envelope (Fig. 3(A)). The most intense Ti $2p_{3/2}$ peak is at 459.2 eV and is due to stable titanium dioxide (TiO_2). This protective TiO_2 barrier protects against further reactions. The presence of fluorine in this titanium matrix is indicated by the emergence of the F $1s$ peak in the S1 spectrum shown in the corresponding Fig. 3(a). When the surface is cleaned by Ar^+ sputter etching, a positive shift in the metal binding energy is

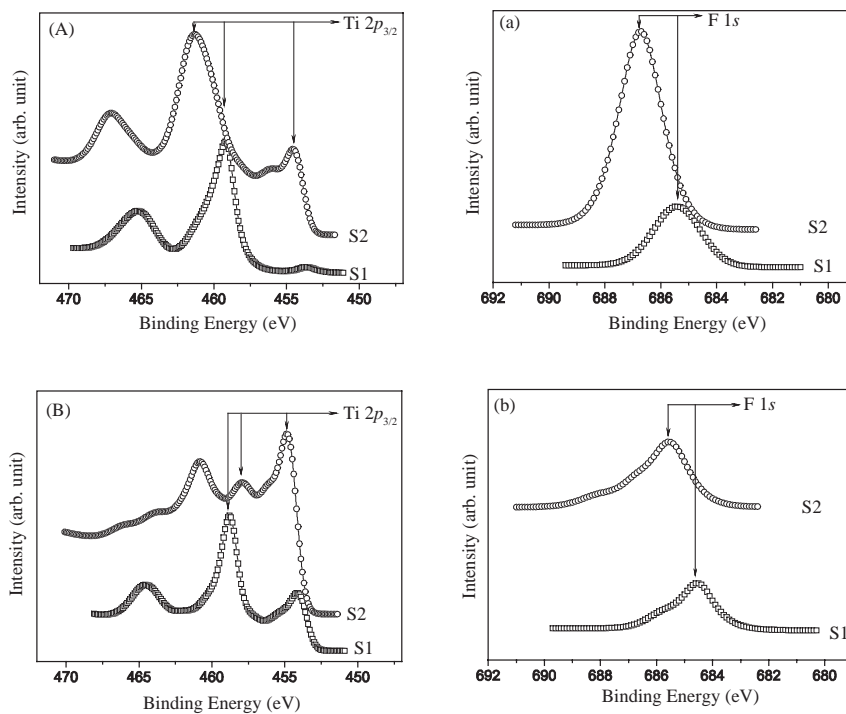


Fig. 3. Ti $2p$ spectra (A, B) and F $1s$ spectra (a, b) obtained from plasma-treated titanium (A-a) and plasma-treated titanium after packaging and firing (B-b). Spectrum S1 is obtained prior to the removal of the native impurities, and spectrum S2 is obtained after *in situ* removal of the native impurities by sputter etching.

observed. This fact is evident in spectrum S2 in Fig. 3(A), where the most intense Ti $2p_{3/2}$ peak is at 461.3 eV. A similar position shift and increase in intensity occur in the F $1s$ spectra shown in Fig. 3(a). The reason for this shifting is rooted in the XPS surface sensitivity and the native oxide envelope. Both oxygen and fluorine are electronegative species, but fluorine has a higher electronegativity than oxygen. In the presence of native oxide on the surface, the metallic binding energy is modulated mainly by oxygen and the effect of fluorine is smaller. Since XPS is a highly surface-sensitive technique, the photoelectrons for the S1 spectrum are mainly obtained from this top impurity layer and very few come from deeper fluorinated titanium. Once this native oxide is removed by Ar^+ sputter etching, the entire spectrum is generated by photoelectrons coming from fluorinated titanium.

The spectra of fired plasma-treated titanium are shown in Fig. 3(B). The titanium surface here is different from that in the previous case because the preparation involves thermal treatment before packaging and high-temperature (500°C) activation after packaging. By packaging, we mean glass-silicon anodic bonding at 400°C under the application of a 200 N force and 650 V. Anodic bonding is an electrochemical process involving the movement of sodium ions, which are considered the predominant carriers of charge away from the interface.⁽¹⁷⁾ This process depletes the region in the glass close to the silicon/glass interface of positive ions, causing it to become negatively charged (with O_2^- anions) and thus producing a large electric field within this region. The bonding proceeds by the formation of Si-O-Si bonds. During this oxidation, free oxygen evolves from the interface and is subsequently trapped in the microcavity. In large, this bonding follows a dry oxidation path. However, the presence of hydroxyl groups from unintentionally dissolved moisture on the glass surface promotes wet chemical oxidation, leading to the evolution of trace amounts of hydrogen. After bonding, the microcavities contain trapped oxygen and occasionally trace levels of hydrogen. Other gases, such as the oxides of carbon (originating from the reaction of oxygen and surface impurity carbon), may be present. The titanium getter may react with these gaseous components during firing, provided it attains the required reaction temperature and presents a clean surface with available reaction sites. The chemical activity of the titanium surface during firing has been analyzed with the help of XPS data (Fig. 3(B)). The first spectrum S1 in Fig. 3(B) depicts mainly the native oxide envelope. After Ar^+ sputter etching, spectrum S2 reveals multiple peaks indicating a significant composition variation in the titanium matrix. The detailed compositional analysis of the surface is discussed with the help of Fig. 4 later. At present, interesting findings are observed in the corresponding fluorine spectra in Fig. 3(b). Spectra S1 and S2, shown in Fig. 3(b), have low intensities and spectrum S2 does not differ much in intensity from S1 even after Ar^+ sputter etching. This implies that a huge loss of fluorine from the titanium matrix has occurred during packaging and the native oxide screening is not significant compared with the spectrum in Fig. 3(a). The development of native oxide on surfaces depends on the surface activity and the availability of unsaturated dangling bonds. If the surface is passive or saturated, atmospheric contaminants have no effect on the surface. It can be indirectly inferred that the thickness of the native barrier formed on the surface is proportional to the level of surface saturation or passivity. Probably, in this case, the fired titanium surface is passive

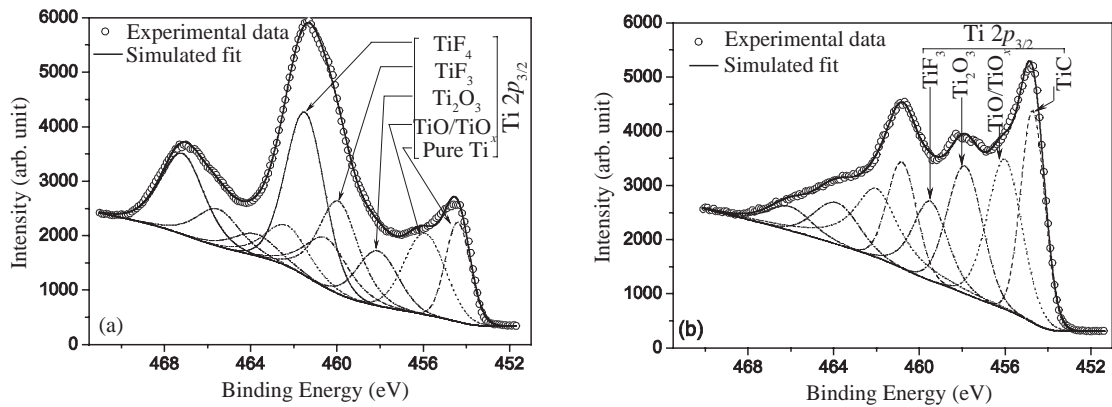


Fig. 4. Detailed Ti $2p$ XPS spectra obtained after *in situ* removal of the native surface impurities from (a) plasma-treated titanium and (b) plasma-treated titanium after packaging and firing. The arrows point to deconvoluted components of the simulated spectrum used to fit the experimental data.

owing to gettering. Consequently, the thin native barrier provided a low level screening and the F $1s$ spectra shown in Fig. 3(b) show a small difference in intensity. The second interesting revelation from Fig. 3(b) is the trailing end of the F $1s$ spectra towards a higher binding energy. In fact, no such trailing end is observed in the F $1s$ spectra of plasma-treated Ti. This asymmetry indicates a different chemical composition of the surface and is discussed in detail in subsequent sections.

For detailed compositional analysis, the Ar⁺ sputter-etched Ti $2p$ spectra have been deconvoluted. The titanium surfaces after plasma treatment and firing are shown in Figs. 4(a) and 4(b), respectively. The plasma-treated spectrum is composed of five distinct chemical states. The first Ti $2p_{3/2}$ peak on the low binding energy side is centered at 454.4 eV and represents pure titanium. The next two Ti $2p_{3/2}$ peaks with low intensities are centered at 456.0 eV and 458.2 eV, and these peaks arise owing to the presence of small amounts of Ti oxides. The peak positions are identical to TiO/TiO_x and Ti₂O₃. The main components of the highest intensity central peak are centered at 461.5 eV and 460.0 eV, which represent the Ti $2p_{3/2}$ binding energies of two important fluorides of titanium, TiF₄ and TiF₃, respectively. These binding energies of 461.5 eV and 460.0 eV are high and are higher than any oxide phase of titanium. Such a location on the high binding energy side is possible owing to the effect of a strong electronegative element having a higher electronegativity than oxygen. Fluorine is present in our system, and it has a higher electronegativity than oxygen. These binding energies definitely belong to the two fluorides, TiF₄ and TiF₃. Since the fluorine content of TiF₄ is greater than that of TiF₃, the binding energy of TiF₄ is greater than that of TiF₃. The remaining peaks in Fig. 4(a) are the Ti $2p_{1/2}$ counterparts of the Ti $2p_{3/2}$ peaks. The combined effect of all the doublet spectra (Ti $2p_{3/2}$ and Ti $2p_{1/2}$) from the components produces the resultant

spectrum, shown as a simulated fit in Fig. 4(a). Among all these peaks, the doublet from TiF_4 has the highest intensity, the probable cause of which is discussed in the context of the reaction mechanism.

Upon packaging and firing the plasma-treated surface, a different surface pattern is observed (Fig. 4(b)). The simulated fit for this situation comprises doublets from four components instead of five. The first one is centered at 454.7 eV and is the Ti $2p_{3/2}$ component belonging to the doublet of titanium carbide (TiC). The next two peaks at 456.1 eV and 457.9 eV correspond to TiO/TiO_x and Ti_2O_3 , respectively. The last Ti $2p_{3/2}$ peak at 459.6 eV is due to the presence of TiF_3 in the fired matrix. Although very small shifts are observed in the binding energies of the compounds in the spectra of fired and prefired samples, no definite shift pattern is apparent. This lack of pattern is probably due to some complicated effect of the interaction between the electronegativities of fluorine and oxygen on the titanium spectrum. There is also the possibility of hydrogen interference in the fired spectrum, as has been discussed earlier. Unfortunately, hydrogen is undetectable by this XPS technique. The striking features of the fired spectrum are the absence of the compound TiF_4 and the increases in the intensities of the oxide phases (Fig. 4(b)). Specifically, the intensity increase of the Ti_2O_3 phase is evident, even in the simulated fit. The elimination of the fluoride component and subsequent increases in intensities of the oxide components are also evident from the comparative F 1s and O 1s spectra of the above two surfaces shown in Figs. 5(a) and 5(b), respectively. The fluorine intensity for the plasma-treated surface, before firing, is very high and is negligible for the fired surface (Fig. 5(a)). In contrast, the oxygen intensity of the plasma-treated surface before firing is lower than that of the fired surface (Fig. 5(b)). Only oxygen is of interest in this comparative study for two reasons. First, the atmosphere between the glass and silicon wafers was purged repeatedly with argon before anodic bonding to eliminate impurities, such as oxygen, nitrogen, and hydrocarbons, from the atmosphere in the cavity. Second, oxygen is the main outgassed impurity during glass-silicon anodic

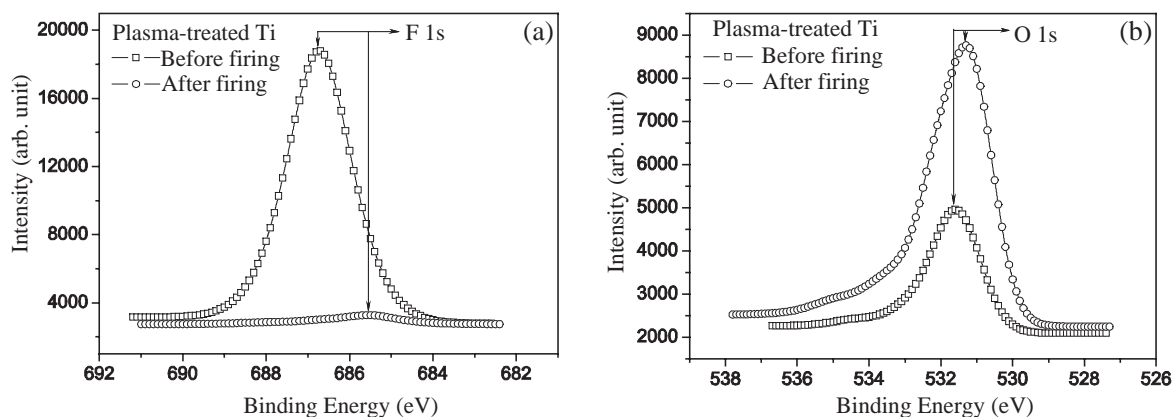


Fig. 5. Comparative XPS spectra before and after firing, obtained after *in situ* removal of native surface impurities: (a) F 1s plasma-treated titanium and (b) O 1s plasma-treated titanium.

bonding, and it must be captured by the getter to maintain the set cavity vacuum. These results definitely indicate that fluorine loss increases the gettering activity of Ti towards oxygen. Generally, the peak area is proportional to the atomic concentration. After appropriate background subtraction and considering the sensitivity factors, the atomic concentrations are calculated using the XPS software. From Table 1, it is seen that the atomic concentrations of oxygen and fluorine increase and decrease, respectively, after firing.

3.2 Carbon residue on titanium surfaces

Carbon contamination on titanium surfaces upon atmospheric exposure is inevitable, and it increases with exposure time. Carbon easily attaches itself along with other foreign elements on the surface and forms a carbonaceous impurity layer. When the titanium surface is treated with a CF_4 -Ar plasma, a fluorocarbon residue is likely to be formed on the surface. Robey *et al.* have reported that the fluorocarbon deposits on a titanium surface due to halocarbon plasma treatment are carbon rich, and there is no indication of the formation of titanium carbide (TiC) on the surface.⁽¹⁸⁾ In the case of titanium, the film residue comprises deposited and fluorinated carbons (CF_x , $x < 4$) with the concentration of the former being higher than that of the latter. The fluorocarbon deposits from the plasma treatment are covered by atmospheric carbon atoms once the surface is exposed to the atmosphere. These fluorocarbon deposits are very difficult to detect, unless *in situ* XPS measurements are carried out after the plasma treatment. The adsorption of these fluorocarbon molecules in the Ti matrix also depends on the thickness of the titanium fluorides (TiF_x , $x = 3$ or 4) on the surface. We speculate that, during the initial stages of fluoride formation, the fluoride layer is thin and the adsorption and subsequent accumulation of fluorocarbons are maximum. With an increase in the thickness of the fluoride layer, the tendency to adsorb is reduced and a surface residue is formed. Ar^+ sputter etching can remove this fluorocarbon residue along with the atmospheric carbon deposits from the surface. However, the trapped carbon and fluorocarbon species are not eliminated by this technique.

The C 1s photoelectron spectra of the plasma-treated sample are shown in Fig. 6(a). The most intense peak in the S1 spectrum is at 284.97 eV, and it is due to elemental carbon. The next two peaks on the high binding energy side are at 286.38 eV and 288.88 eV. These peaks are due to adsorbed carbon-oxygen (C/O) species, such as C=O and O-C=O functional groups. After Ar^+ sputter etching, these carbon atoms are completely

Table 1

Atomic concentrations of fluorine and oxygen in plasma-treated titanium before and after firing.

	Plasma-treated Ti	
	Fluorine	Oxygen
Before firing (B)	55.16%	14.61%
After firing (A)	2.59%	45.92%
Difference (A–B)	–52.57%	+31.31%

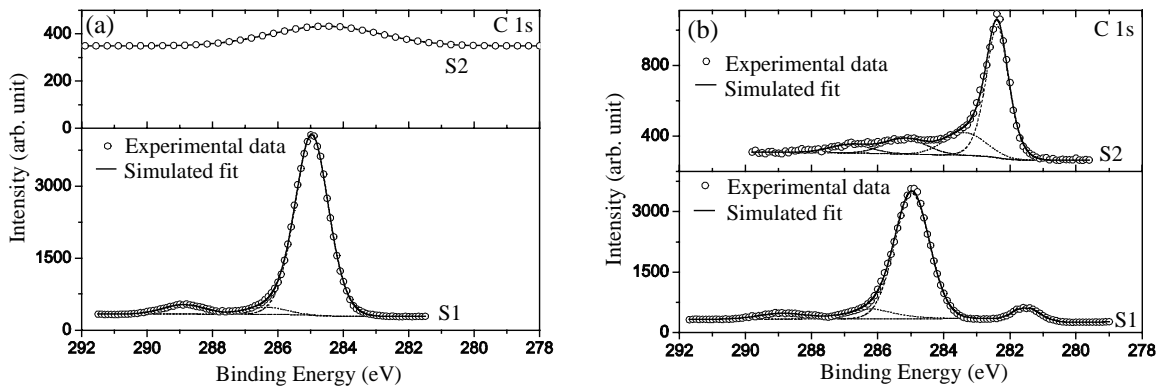


Fig. 6. Detailed C 1s XPS spectra from (a) plasma-treated titanium and (b) plasma-treated titanium after packaging and firing.

removed from the surface. Although the surface is then considered to be clean, a small hump with a very low intensity exists at 284.4 eV in the S2 spectrum of Fig. 6(a). This hump in the C 1s spectra arises owing to the trapped carbon residue in the deeper layers. Basically, XPS is a surface-sensitive technique and the well-defined peaks are due to electrons that have not suffered inelastic energy loss while emerging from the sample. Electrons that have lost energy increase the level of the background instead of showing a prominent peak. The absence of any peak in S2 at approximately 281–282 eV indicates that there is no TiC on the surface after plasma treatment (Fig. 6(a)). Nevertheless, the C 1s spectrum (S1) of the plasma-treated titanium surface after firing reveals a small carbide peak at 281.6 eV (Fig. 6(b)). This carbide is formed by the reaction of the carbon residue with titanium during the high-temperature packaging process. The rest of the S1 spectrum in Fig. 6(b) includes an intense peak at 284.96 eV and two low intensity peaks at 286.21 eV and 288.9 eV. These three peaks are adventitious carbon contaminants due to atmospheric exposure and are not an integral part of the fired matrix. Upon cleaning the surface with Ar⁺ sputter etching, these secondary carbon impurities are eliminated and the C 1s spectrum (S2) of the real surface is revealed (Fig. 6(b)). The intense peak at 282.38 eV in S2 is the carbide phase. This carbide component has been observed earlier in the detailed Ti 2p spectrum of fired Ti (Fig. 4(b)). The position difference (~ 0.78 eV) of this peak between the S1 and S2 spectra is probably due to Ar⁺ sputtering, which may introduce interstitial defects in the TiC lattice.⁽¹⁹⁾ The asymmetry of this carbide peak towards the high binding energy side is also attributed to the presence of a ternary composite of Ti, F, and C, which yields the second peak at 283.36 eV. The last two small peaks at 285.17 eV and 286.83 eV in the S2 spectrum can be assigned to some free and polymer-like carbons present on the fired surface.

3.3 Colour and morphology

The colours of plasma-treated titanium before and after firing are shown in Figs. 7(A) and 7(B), respectively. The plasma-treated titanium before firing has a uniform whitish appearance. However, the colour of plasma-treated titanium after firing is bluish violet. This colour change is due to TiF_3 , because commercially available titanium (III) fluoride is a crystalline solid with a violet colour. The surface morphology of the above two samples revealed by FE-SEM is shown in Figs. 7(a) and 7(b), respectively. The plasma-treated titanium surface has unevenly distributed white spots on a uniform background. This is possibly due to scattered carbon particles in the residue left on the surface after plasma etching. Sometimes, micro/nanoundulations on a glass substrate may leave similar imprints on the titanium film. Therefore, the colour contrast on a plasma-treated Ti surface may be a combined effect of carbon residue and irregularities on the glass substrate. The fired surface does not reveal any special morphological characteristics (Fig. 7(b)). The overall brightness of the surface is uniform. Basically, the fired surface is a composite of TiC , TiO , Ti_2O_3 , and TiF_3 . In a composite surface like this, the manifestation of a particular grain orientation is highly unlikely. It can be predicted that the surface has a very fine grain structure with randomly oriented grains. Owing to experimental limitations, further image magnification has not been possible.

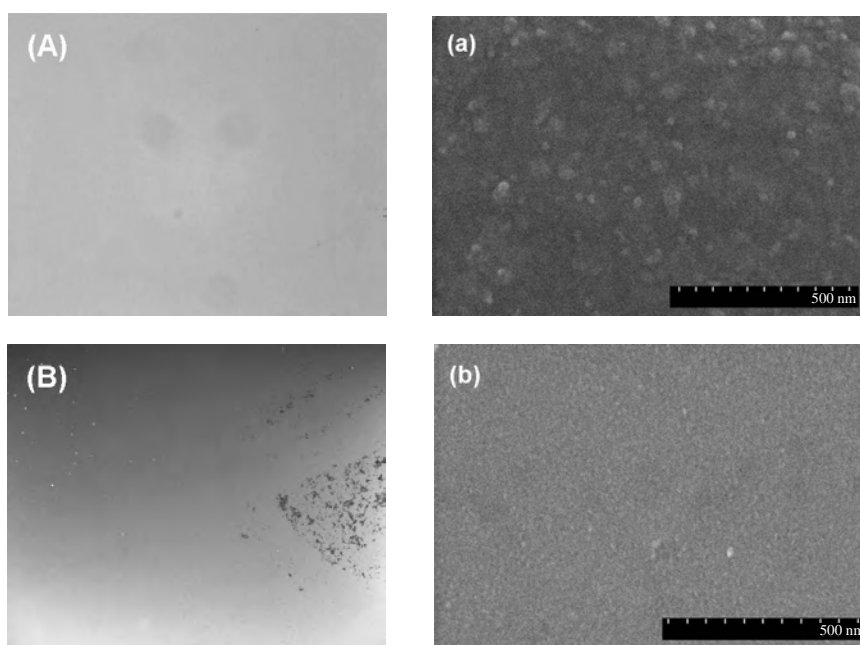


Fig. 7. Optical (A, B) and SEM (a, b) images obtained from plasma-treated titanium (A-a), and plasma-treated titanium after packaging and firing (B-b).

4. Discussion

4.1 Reaction and mechanism of gettering

For plasma treatment, tetrafluoromethane (CF₄) was selected because titanium halide binary compounds all have relatively high vapour pressures compared with other titanium compounds.⁽²⁰⁾ The halocarbons are also relatively easy to handle because of their noncorrosive properties and low toxicity. Our objective was to etch the top stoichiometric native TiO₂ layer and subsequently fluorinate the Ti matrix.

The plasma composition can be realized on the basis of the following equations.



Other ionization reactions in addition to those in eq. (1) are also possible in the plasma. Sometimes, trace levels of oxygen present in a plasma chamber may participate in the spontaneous generation of atomic fluorine as shown below.



This plasma has two parts, i.e., a reactive part consisting of fluorocarbon and fluorine species, and a passive part consisting of argon atoms/ions. The role of the reactive part is to chemically attack the titanium, while the passive part has abrasive or erosive properties. Simultaneous attack on the top native stoichiometric oxide layer (TiO₂) by reactive and passive parts gradually increases the nonstoichiometry (TiO_x, $x < 2$). This continues until a pure Ti surface is exposed, at which point the etching rate increases. The two important reaction products of the interaction of fluorine and titanium are titanium (IV) fluoride (TiF₄) and titanium (III) fluoride (TiF₃). After the plasma process is over, the surface is covered by a highly fluorinated layer composed of TiF₄ and TiF₃; the former is more volatile than the latter. The sublimation temperature of TiF₄ is 284°C, while TiF₃ sublimates between 486 and 592°C.^(21,22) The two fluorides are stable at room temperature. The simultaneous existence of TiF₄ and TiF₃ is also clear from Fig. 4(a) and the high fluorine-to-titanium atomic ratio (F/Ti > 3) obtained after XPS spectrum deconvolution. The high intensity of TiF₄ in Fig. 4(a) obviously indicates that TiF₄ formation is more favourable than TiF₃. Ramanath *et al.* reported that when Ti is exposed to WF₆ gas at 445°C, TiF₃ is formed first owing to the low kinetic barrier of the reaction. Under the influence of high WF₆ partial pressure, TiF₃ is subsequently converted to TiF₄.⁽²³⁾ Generally, fluorine reacts with Ti and TiO₂ at high temperatures (200–350°C) to yield titanium fluoride.⁽²⁴⁾ However, under the influence of the reactive plasma, which is more powerful than simple molecules, fluoride formation is possible even at room temperature. Therefore, in this study, the first reaction product is expected to be TiF₃. Since fluorine partial pressure is also very high because of the plasma composition (60%CF₄+40%Ar), TiF₃ is converted to TiF₄ spontaneously and forms the

top protective layer of the plasma-treated Ti. The reaction sequence is as follows.



Adding eqs. (3.1), (3.2), and (3.3),



The formation of TiF_4 on the surface saturates the reactivity of the surface to the plasma at room temperature and therefore may stop the effect of the plasma treatment, unless there is another way to supply more Ti atoms from the bulk Ti matrix at room temperature. With this experimental data, it is difficult to substantiate the occurrence of Ti migration from the bulk to the surface at room temperature.

Commercially available TiF_4 and TiF_3 are white and violet, respectively, under visible light. Therefore, the colour of Ti after plasma treatment is not affected by violet-coloured TiF_3 as it is covered by a white TiF_4 layer (Fig. 7(A)).

The sample with the indicated surface characteristics is brought outside the plasma chamber for the glass-silicon packaging process. Atmospheric contaminants, such as oxygen and carbon, stick to the surface to form a native protective layer. Since the TiF_4 layer is present on the Ti surface, the native layer is formed on the TiF_4 surface without coming in contact with titanium. The first step of this packaging process is sample outgassing by temperature, vacuum, and argon purging, as described in "Materials and Methods." During this thermal outgassing process, the TiF_4 layer disintegrates owing to its high vapour pressure and tendency to sublime from the surface. Because it is sandwiched between the top native impurity layer and the bulk Ti, the sublimation of the TiF_4 layer helps desorb native impurities from the titanium surface at the same time. The gases are expelled out of the cavity by the high-vacuum pumping of the bonding machine. This process yields a clean titanium surface. This statement is substantiated by the huge reduction in fluorine atomic concentration (Fig. 5(a), Table 1) and the presence of only TiF_3 after firing (Fig. 4(b)). The existence of TiF_3 is also evident from the change in getter colour to violet after packaging (Fig. 7(B)). In fact, TiF_3 is a nonvolatile fluoride of Ti and does not sublime in the temperature range of packaging.⁽²²⁾ The loss of fluoride and native impurities exposes a highly reactive Ti surface that captures outgassed oxygen from anodic bonding.

5. Conclusions

This work outlines the gettering activity of CF_4 -Ar plasma-treated titanium within anodically bonded microcavities. The native oxide impurity on the titanium surface, which is a hindrance to efficient oxygen capture during firing, is eliminated before getter

firing. However, the compounds TiC and TiF₃ in the fired getter are difficult to eliminate with this packaging process. Nevertheless, the concentration of surface-trapped oxygen after firing is high. XPS measurements reveal that titanium does not reach its final oxidation state (Ti⁴⁺) because TiO₂ is not detected on the fired surface. Therefore, the getter surface after firing is still unsaturated and is capable of further oxygen capture during long-term outgassing of glass microcavities. All these results indicate that halocarbon-plasma-treated titanium can be used as a potential getter to create a very low-pressure environment within vacuum-packaged inertial sensors for an enhanced device performance.

Acknowledgement

Surajit Kumar Hazra gratefully acknowledges the support provided by the BK-21 program of South Korea for the period 2007–2008.

References

- 1 D. R. Sparks, S.-M. Ansari and N. Najafi: IEEE Trans. Adv. Pack. **26** (2003) 277.
- 2 K. M. Welch: J. Vac. Sci. Technol., A **21** (2003) S19.
- 3 T. A. Giorgi: Jpn. J. Appl. Phys. **2** (1974) 53.
- 4 T. A. Giorgi, B. Ferrario and B. Storey: J. Vac. Sci. Technol., A **3** (1985) 417.
- 5 K. Ichimura, K. Ashida and K. Watanabe: J. Vac. Sci. Technol., A **3** (1985) 346.
- 6 K. Ichimura, M. Matsuyama and K. Watanabe: J. Vac. Sci. Technol., A **5** (1987) 220.
- 7 C. Boffito, B. Ferrario, P. della Porta and L. Rosai: J. Vac. Sci. Technol., A **18** (1981) 1117.
- 8 X. Liu, P. K. Chu and C. Ding: Mater. Sci. Eng., R **47** (2004) 49.
- 9 C. Leyens, F. Kocian, J. Hausmann and W. A. Kaysser: Aerosp. Sci. Technol. **7** (2003) 201.
- 10 J. Zemek and P. Jiricek: Vacuum **71** (2003) 329.
- 11 M. Esashi, S. Sugiyama, K. Ikeda, Y. Wang and H. Miyashita: Proc. IEEE **86** (1998) 1627.
- 12 B. Lee, S. Seok and K. Chun: J. Micromech. Microeng. **13** (2003) 663.
- 13 F. Rosebury: Handbook of Electron Tube and Vacuum Techniques, AIP, 1993, p. 16.
- 14 D. Lichtman and T. R. Kirst: J. Vac. Sci. Technol., A **3** (1966) 224.
- 15 H. Henmi, S. Shoji, Y. Shoji, K. Yoshimi and M. Esashi: Sens. Actuators, A **43** (1994) 243.
- 16 Y. Mizuno, F. K. King, Y. Yamauchi, T. Homma, A. Tanaka, Y. Takakuwa and T. Momose: J. Vac. Sci. Technol., A **20** (2002) 1716.
- 17 K. M. Knowles and A. T. J. van Helvoort: Int. Mater. Rev. **51** (2006) 273.
- 18 S. W. Robey, M. A. Jaso and G. S. Oehreien: J. Appl. Phys. **65** (1989) 2951.
- 19 G. Li and L. F. Xia: Thin Solid Films **396** (2001) 16.
- 20 C. J. Mogab and T. A. Shankoff: J. Electrochem. Soc. **124** (1977) 1766.
- 21 Handbook of Chemistry and Physics, 63rd ed. (CRC, Boca Raton, FL, 1982–1983), p.b. 95.
- 22 K. F. Zmbov and J. L. Margrave: J. Phys. Chem. **71** (1967) 2893.
- 23 G. Ramanath, J. E. Greene, J. R. A. Carlsson, L. H. Allen, V. C. Hornback and D. J. Allman: J. Appl. Phys. **85** (1999) 1961.
- 24 H. M. Haendler, S. F. Bartram, R. S. Becker, W. J. Bernard and S. W. Bukata: J. Am. Chem. Soc. **76** (1954) 2177.